23rd International Conference on
Harmonisation within Atmospheric Dispersion Modelling
for Regulatory Purposes
15-19 September 2025, Hamburg, Germany

EXTENDED ABSTRACT

Non-dimensional eddy diffusivity within buoyant plumes in a turbulent boundary layer based on a wind tunnel study

Miaoyan Pang[1,2], [1]Centre for Wind, Waves, and Water, The University of Sydney, Sydney, NSW, Australia, [2] Karlsruhe Institute of Technology, Institute for Water and Environment (IWU), Laboratory of Building and Environmental Aerodynamics, Karlsruhe, Germany

miaoyan.pang@sydney.edu.au

Kapil Chauhan, Centre for Wind, Waves, and Water, The University of Sydney, Sydney, NSW, Australia

Krishan Talluru, School of Engineering and Technology, UNSW Canberra, Campbell, ACT 2612, Australia

Introduction

The transport equation is the governing equation for phenomena such as stack emissions. Assuming steady flow and molecular diffusion is negligible compared to turbulent diffusion, the Reynolds-averaged transport equation can be simplified to:

$$U_i \frac{\partial C}{\partial x_i} + \frac{\partial \overline{u_i c}}{\partial x_i} = 0$$

where U_i is the mean velocity, u_i is the velocity fluctuation about the local mean, C is the mean concentration, and c is the concentration fluctuation. In this manuscript, x and u are in the streamwise direction, z and w are in the vertical direction, and y and v are in the spanwise direction. Even if the velocity statistics are known a priori, the above equation cannot be solved for C, since the scalar flux terms, $\overline{u_i c}$, are unknown. Experimental data are valuable in prior estimation of the scalar flux terms, especially if they can be underpinned within a similarity formulation. Often, a simple approach to model the scalar fluxes is to relate them linearly to the mean concentration gradient as $\overline{u_i c} = \kappa_i \left(\frac{\partial C}{\partial x_i}\right)$, where κ_i is a dimensional eddy diffusivity. This model is also known as the gradient-diffusion approach, employed by Csanady (1967) and Sykes *et al.* (1986), for example. A drawback of κ_i is that it is dimensional and varies with downstream distance, even if source and background flow conditions do not vary (see figure 10(a) in Vanderwel and Tavoularis (2014)). Non-dimensional representation of eddy diffusivity is not yet linked to any of the self-similar characteristics of the plume. This extended abstract presents a scaling law of vertical scalar fluxes based on wind tunnel studies of neutrally, positively, and negatively buoyant plumes.

Since the order of magnitude of $\frac{\partial \overline{wc}}{\partial z}$ is much higher than that of $\frac{\partial \overline{uc}}{\partial x}$ for the development of the plume, the focus of this manuscript will be on $\overline{wc}$. The theoretical shape of $\overline{wc}$ of an elevated source can be diagnosed by considering that $\overline{wc}$ at the plume centreline due to symmetry and far away outside the plume as concentration vanishes (Wyngaard, 2013). The location of the plume centreline, z_0, is defined as the height of the maximum root mean square (RMS) concentration, $\sigma_{c,0}$, in this abstract. Packets of concentration $(+c)$ moving upwards $(+w)$ and negative concentration fluctuations $(-c)$ moving downwards $(-w)$ result in $\overline{wc} > 0$ above the plume centreline (Wyngaard, 2013). Similarly, $\overline{wc}$<0 below the plume centreline. Overall, the profile has an S-shape.

Wind Tunnel Experiments

A comprehensive description of the experimental setup and parameters is provided in (Pang *et al.*, 2025). Here, the most relevant experimental details are summarised. The experiments were conducted in the Boundary Layer Wind Tunnel at the University of Sydney. A turbulent boundary layer, with a freestream of 2.5 m/s, was generated using LEGO baseboards positioned 12 m upstream of the test section, resulting in a boundary layer thickness (δ) of 255 mm. No roughness was installed in the test section. The boundary layer Reynolds number (Re_δ) was 43,100, and the friction Reynolds number (Re_τ) was 1,600. Point sources were positioned at heights of 0.16δ and 0.32δ. The source velocity equals the local mean velocity in the background. The released gas mixture consisted of 1.5% iso-butylene (tracer gas) and 98.5% carrier gas. The carrier gases—Helium, Nitrogen, or Argon—were used to modulate the density of the source gas mixtures. Vertical measurements were performed at δ, 2δ, and 4δ downstream of the release point. Table 1 documents the configurations of source conditions, along with their corresponding legends. Simultaneous concentration and velocity measurements were acquired using a photo-ionisation detector (PID) manufactured by Aurora Scientific and a 55P61 x-wire probe from Dantec Dynamics. The PID, with its high-frequency response of 300 Hz, measured concentration fluctuations and allowed for cross-correlation with the ×-wire measurements of streamwise and vertical velocity components.

Vertical Scalar Fluxes

Figure 1(a) presents the vertical scalar flux distributions $(\overline{wc})$ for two elevated sources as a function of normalised height (z/δ). The legends are summaries in table 1. The observed trends align with theoretical predictions and previous experimental findings, exhibiting positive values above the plume centreline and negative values below. As anticipated, the overall magnitude of $\overline{wc}$ diminishes with increasing downstream distance. Additionally, asymmetry exists between the upper and lower plume regions due to the variation in vertical velocity fluctuation profiles. Since wall-normal velocity fluctuations influence the local scalar flux magnitude, $\overline{wc}$ is normalised using the respective RMS values (σ_w and σ_c) in figure 1(b). Although not presented here, we find that normalising using σ_c gives a superior collapse compared with normalising with C. This improvement likely stems from the fact that $\overline{wc}$ is a second-order cross-moment linked to the second-order moment of concentration. For the normalisation of height, the classical Gaussian plume model is employed. The σ_c profiles for elevated sources conform well to the

Gaussian plume model, consistent with previous experimental investigations, as demonstrated in figure 2(a), where the vertical axis plots $\xi_\sigma = (z - z_0)/\delta_\sigma$, the distance relative to the centreline height normalised by the half-width of the RMS concentration profile (δ_σ). This same ξ_σ is plotted against $\overline{wc}/\sigma_w\sigma_c$ in figure 1(b). The experimental data collapse reasonably well and is anti-symmetric about the plume centreline ($\xi_\sigma = 0$), revealing the theoretical S-shaped profiles discussed in the introduction. Furthermore, figure 2(b) highlights that the gradient of the Gaussian model ($\partial(\sigma_c/\sigma_{c,0})/\partial\xi_\sigma$) also has an S-shaped behaviour. The gradient exhibits a linear relationship with the normalised scalar flux, as illustrated in figure 2(c). Importantly, this relationship remains invariant across different downstream distances and source conditions, enabling the formulation of a generalised model:

$$\frac{\overline{wc}}{\sigma_c\sigma_w} = \gamma_z \times \frac{\partial(\sigma_c/\sigma_{c,0})}{\partial\xi_\sigma}. \qquad 1$$

Here γ_z is a non-dimensional parameter that is approximately constant, evidenced by the constant slopes in figure 2(c). Note that γ_z is not the well-known dimensional eddy-diffusivity, as it is not acting on the mean concentration gradient. Two fundamental assumptions underpin the model development. The elevated source assumption eliminates wall interaction effects, while the thin plume assumption requires that the plume width remains much smaller than both the distance from the source and the boundary layer thickness. Under the latter condition, velocity shear and fluctuations across the vertical plume extent are approximately constant.

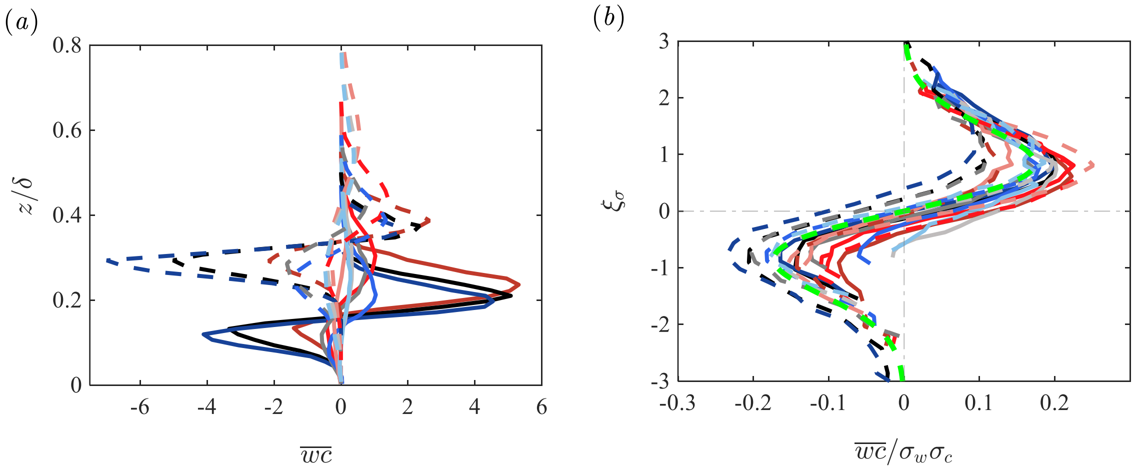

Figure 1. (a) vertical scalar fluxes (b) vertical scalar fluxes normalised by the RMS of concentration and vertical velocity fluctuation. measured at three downstream distances. The dashed green line is the right-hand side of equation 1. For legends see table 1.

	Measurement location	Positively buoyant	Neutrally buoyant	Negatively buoyant
Source height = 0.16δ	δ	—	—	—
	2δ	—	—	—
	4δ	—	—	—

Source height = 0.32δ	δ			
	2δ			
	4δ			

Table 1.Legends for all figures. Red, black, and blue colours correspond to different buoyancy cases, with darker shades indicating shorter downstream distances. Solid and dashed lines represent the two source heights investigated. δ is the boundary layer thickness.

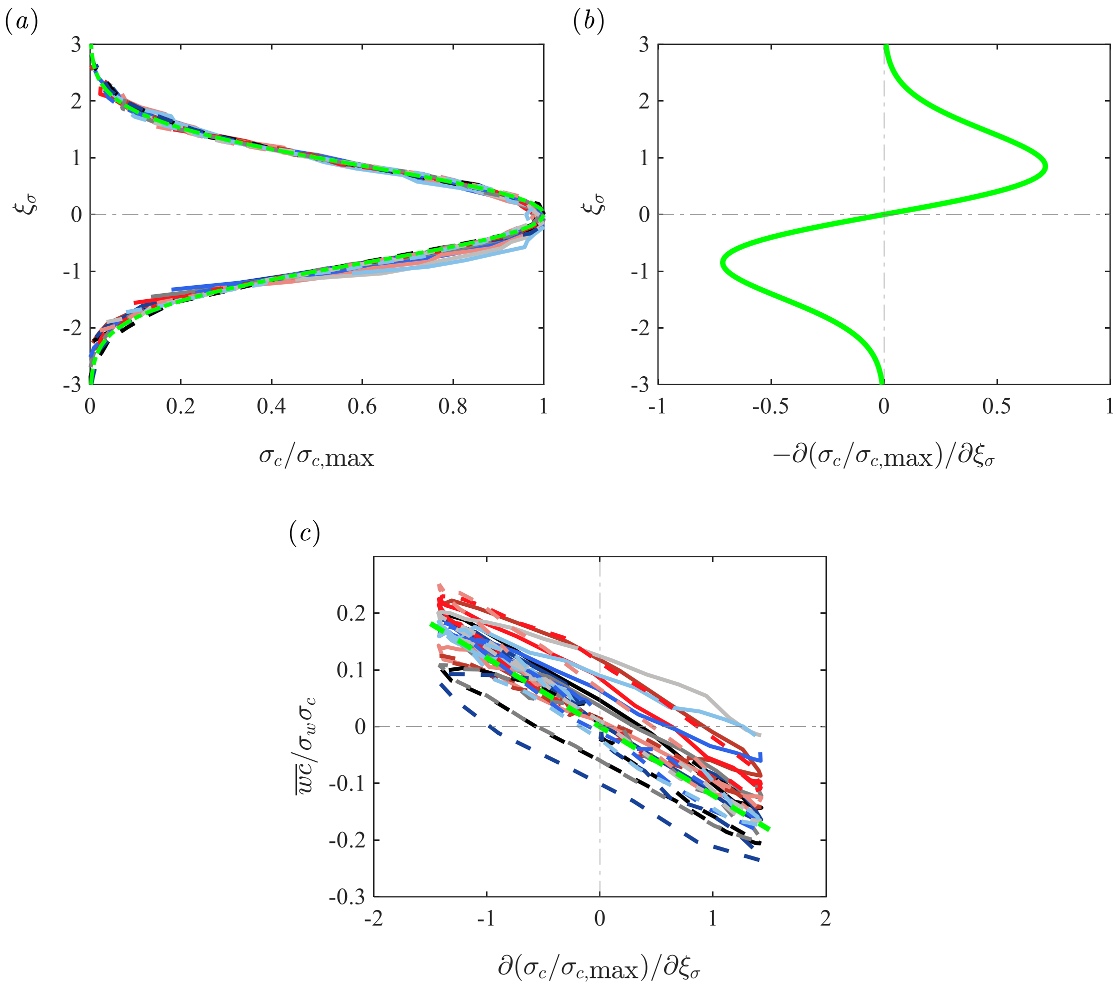

Figure 2. (a) RMS of concentration profiles described by the Gaussian model, represented by the green dash-dotted line. (b) Derivative of the Gaussian model. (c) Normalised fluxes plotted against the derivative of the Gaussian model. The green dashed line here is the line of best fit, whose slope is γ_z in equation 1. For legends, see Table 1.

The intercepts observed in figure 2(c) warrant further discussion. Investigation reveals no apparent correlation between these intercepts and either buoyancy effects or downstream distance. The individual intercepts exhibit scatter around a mean value of approximately zero, suggesting that the observed variations in intercepts are most likely attributable to experimental uncertainty. However, buoyancy does play a role here by changing z_0, the height of maximum σ_c, and δ_σ, the plume width calculated from the profile of σ_c. This discrepancy caused by buoyancy is distinguished in figures 2(a) and 2(c) for the same reason -- the introduction of ξ_σ.

The intercepts shown in Figure 2(c) merit additional discussion. A systematic investigation reveals no discernible correlation between these intercepts and either buoyancy effects or downstream distance. Instead, the individual intercepts scatter about a mean that is essentially zero, indicating that the observed variability is most likely due to experimental uncertainty. Buoyancy does influence the measurements indirectly, however, by altering z_0 (the height at which σ_c attains its maximum) and δ_σ (the plume width inferred from the σ_c profile). This buoyancy-induced discrepancy disappears in Figures 2(a) and 2(c) because the introduction of the normalised coordinate ξ_σ effectively removes the dependence on z_0 and δ_σ.

Conclusion and Discussion

Understanding scalar flux behaviour provides critical insights into plume dispersion within turbulent flows. This study introduces a novel scaling law that relates vertical scalar fluxes to the gradient of RMS concentration profiles. Experimental analysis demonstrates that the ratio of normalised scalar fluxes and the gradient remains approximately constant, yielding a non-dimensional parameter, γ_z. γ_z differentiates from the dimensional eddy diffusivity based on the mean concentration gradient. This empirical relationship offers a simple framework for model verification, independent of source conditions or boundary layer characteristics. Future investigations should explore the potential for utilising γ_z to predict plume evolution. Additionally, the applicability of RMS-normalised flux scaling to dispersion over rough surfaces warrants further examination to extend the model's utility across diverse environmental conditions.

References

Csanady, G. T. (1967) ‘Concentration Fluctuations in Turbulent Diffusion’, Journal of Atmospheric Sciences, *24*(1), 21-28.

Pang, M., Chauhan, K. and Talluru, K. M. (2025) ‘Measurements of buoyant plumes in a turbulent boundary layer’, Experiments in Fluids, 66(10). doi: 10.1007/s00348-024-03941-7.

Sykes, R. I., Lewellen, W. S., and Parker, S. F. (1986) ‘A Gaussian Plume Model of Atmospheric Dispersion Based on Second-Order Closure’, Journal of Climate and Applied Meteorology, 25(3), 322–331.

Vanderwel, C., and Tavoularis, S. (2014) ‘Measurements of turbulent diffusion in uniformly sheared flow’. Journal of Fluid Mechanics, 754, 488–514.

Wyngaard J. C. 2013, Turbulence in the Atmosphere, Cambridge University Press.